applied sciences

MDPI

Article

Numerical Simulation of Hot Jet Detonation with Different Ignition Positions

Hongtao Zheng, Shizheng Liu, Ningbo Zhao *, Xiang Chen, Xiongbin Jia and Zhiming Li

College of Power and Energy Engineering, Harbin Engineering University, Harbin 150001, China; zhenghongtao9000@163.com (H.Z.); liushizheng1990@163.com (S.L.); chenxiang344@163.com (X.C.); xiongbinjia@hrbeu.edu.cn (X.J.); lizhimingheu@126.com (Z.L.)

* Correspondence: zhaoningbo314@hrbeu.edu.cn; Tel.: +86-0451-8251-9647

Received: 23 September 2019; Accepted: 27 October 2019; Published: 29 October 2019

Abstract: Ignition position is an important factor affecting flame propagation and deflagration-to-detonation transition (DDT). In this study, 2D reactive Navier–Stokes numerical studies have been performed to investigate the effects of ignition position on hot jet detonation initiation. Through the stages of hot jet formation, vortex-flame interaction and detonation wave formation, the mechanism of the hot jet detonation initiation is analyzed in detail. The results indicate that the vortexes formed by hot jet entrain flame to increase the flame area rapidly, thus accelerating energy release and the formation of the detonation wave. With changing the ignition position from top to wall inside the hot jet tube, the faster velocity of hot jet will promote the vortex to entrain jet flame earlier, and the DDT time and distance will decrease. In addition, the effect of different wall ignition positions (from 0 mm to 150 mm away from top of hot jet tube) on DDT is also studied. When the ignition source is 30 mm away from the top of hot jet tube, the distance to initiate detonation wave is the shortest due to the highest jet intensity, the DDT time and distance are about 41.45% and 30.77% less than the top ignition.

Keywords: hot jet detonation initiation technique; flame acceleration; detonation combustion; vortex; ignition position

1. Introduction

Detonation combustion has attracted plenty of attention from researchers because of its high thermal efficiency, low entropy generation and self-pressurization characteristic [1,2]. According to the formation process of detonation waves and operating characteristics in the engines, detonation engines can be divided into rotating detonation engine (RDE) [3,4], pulse detonation engine (PDE) [5,6] and standing detonation wave engine (SDWE) [7]. The detonation initiation technology is one of the bottlenecks and key technologies that restrict the engineering application of any detonation engines.

The common detonation initiation techniques are mainly divided into two categories: one is direct detonation, and the other is indirect detonation initiation. Compared with direct detonation, indirect detonation initiation requires less ignition energy, thus becoming the main direction of the detonation domain. A weak energy ignition source triggers combustion and then leads to a transition to detonation through the accumulation of energy, which is a commonly used indirect detonation initiation method [8]. Deflagration-to-detonation transition (DDT) usually requires a transition distance. However, too long transition distance may cause oversize engines and performance loss. Therefore, it is necessary to explore suitable short-range detonation initiation technology [9]. In published literature, studies have been done on detonation initiation mechanism and enhancement approach, such as hot jet [10,11], solid obstacle [12,13], fluidic obstacle [14,15], plasma [16] and shock focusing detonation initiation technology [17].

Especially, the hot jet detonation initiation firstly forms a high-energy flame in the jet tube, and then the jet flame rapidly forms a high-intensity turbulent flame in the detonation chamber, eventually forming a detonation wave in a short distance. Since the hot jet detonation initiation is an effective detonation technique with short distance and low flow loss, it is one focus of current research. Shimada et al. [18] firstly applied the hot jet tube on the detonation chamber to achieve a reliable detonation. Through visual experiments, it was found that a hot jet could quickly form a turbulent flame at the head of the detonation chamber and promote the formation of a detonation wave. Zhao et al. [19] used the numerical simulation method to study the hot jet detonation initiation, their results showed that the energy provided by the hot jet was 20 times that of the spark, and the hot jet technology could effectively reduce the initiation distance of DDT. Other literature got the same conclusion by experiments [20,21]. Subsequently, plenty attention had been poured on effect of jet intensity on DDT. Lots of research had been investigated jet intensity by changing the structure of the hot jet tube, and the same conclusion was obtained that the initiation time and distance of DDT were short when the jet intensity is sufficient [22–25]. Using ethylene/oxygen with nitrogen diluted, He et al. [26] explored the effects of different jet velocity on DDT distance. From their experimental results, it was clearly seen that jet velocity played an important role in accelerating DDT, the faster jet velocity the shorter DDT distance. Wang et al [27] numerically investigated propane/air hot jet detonation initiation process by changing the length of jet tube, it was found that the increasing length of jet tube resulted in faster jet velocity, thus decreasing the initiation time and distance of DDT.

According to the review of previous work, it is concluded that the faster jet flame velocity was, the shorter DDT distance. Up to now, the common method to obtain fast jet flame was increasing the length of jet tube. However, too long length of the hot jet tube would increase the formation time of hot jet and increase the DDT time, so that the performance of the engines was seriously affected. In addition, oversize was inconvenient for practical applications. So, alternatives to increase the length of hot jet tubes needed to be explored. Previous studies had shown the ignition position inside the detonation chamber was an important factor in flame propagation and formation of DDT [28–30]. Peng and Weng [31] numerically investigated the effects of different ignition position on DDT. They indicated that wall ignition had advantages over closed-end ignition in the initiation time and distance of DDT. Blanchard et al. [32] studied the effects of different wall ignition positions on flame propagation and DDT by hydrogen/air experiments. The results showed that the expansion of burnt fuel against the closed section of the tube behind flame front increased flame speed and turbulence when the ignition position was a certain distance from the closed section. From these studies of the ignition position, it was clearly seen that ignition position inside the detonation chamber had a great influence on the detonation initiation time and distance, and wall ignition was more conducive to flame acceleration. Using this principle, optimization of the ignition position inside the jet tube may also obtain a fast jet velocity to reduce the detonation distance without changing the length of the jet tube. However, the influence of the different ignition positions inside the jet tube on hot jet detonation initiation had not been fully studied and needed more detailed analysis and discussion.

Motivated by the above considerations, the present study performs the 2D numerical simulations to investigate the effect of different ignition positions inside the hot jet tube on DDT. Firstly, the mechanism of hot jet detonation initiation and flow characteristics are analyzed in detail through the study of the vortex-flame interaction, temperature, pressure, and velocity. Secondly, the jet parameters and flame acceleration performance of top and wall ignition are compared to investigate the reasons why wall ignition is more favorable for DDT. Finally, the wall ignition position is further optimized, it expects to lay the foundation for the design and application of the efficient and compact hot jet detonation initiation device.

2. Numerical Model and Methods

2.1. Physical Model

Figure 1 presents the physical model of the detonation chamber analyzed in this paper. As shown in the Figure, the chamber is 100 mm in diameter and 1800 mm in length, and the left wall of the detonation chamber is closed. Six obstacles are arranged inside the detonation chamber which the blocking ratio is 0.35 [33]. The distance between the first obstacle and the left wall of the detonation chamber is 380 mm. The previous three obstacles are equidistant, the distance between adjacent obstacles is 175 mm. The distance between the last three obstacles is 250 mm. Four monitoring points (P1–P4) are set to monitor the changing of parameter. The monitoring point is 100 mm behind the obstacle. The hot jet tube with the 32 mm inner diameter and the 200 mm length is aligned perpendicular to the centerline of the detonation chamber. The distance between the hot jet tube and the left wall of the detonation chamber is 114 mm, the ignition is located in the hot jet tube. As shown in Figure 1b, top ignition or wall ignition will be investigated. Flame accelerates in hot jet tubes first, and then jet flame propagates into detonation chamber and produces a detonation wave in it.

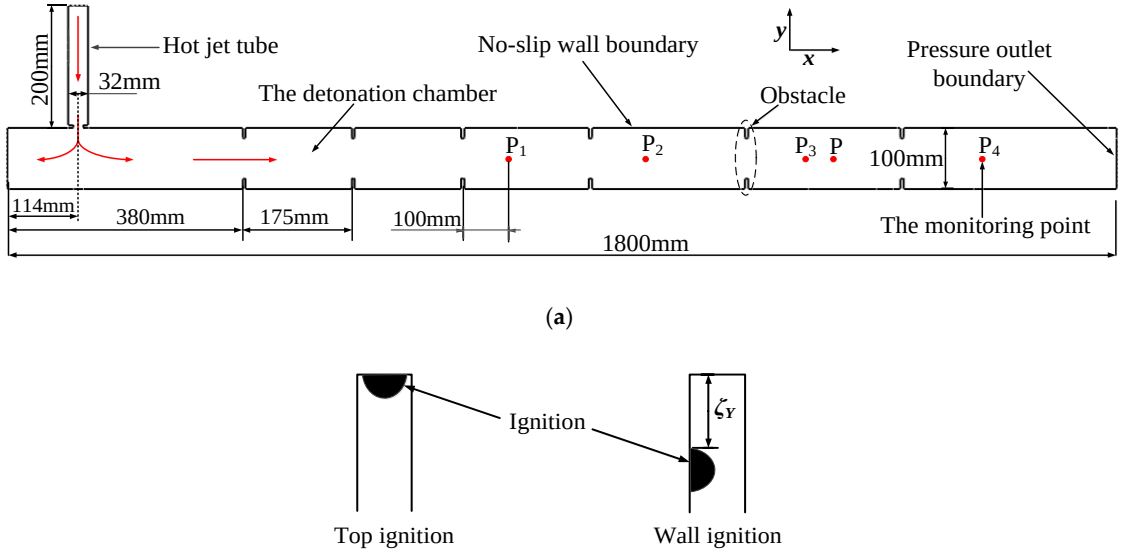

Figure 1. Schematic of geometry, (**a**) computational domain and (**b**) ignition position.

2.2. Numerical Method

In this study, the numerical simulations are performed using ANSYS Fluent software. The calculation is solved on the basis of two-dimensional Navier-Stokes equations for a viscous compressible gas coupled with chemical kinetics and the equation of state of ideal gas. The vertical jet tube causes obvious shear flows in the detonation chamber, so SST k-ω turbulence model is employed which defines the transport of the turbulence shear stress in the turbulent viscosity to resolve the unsteady turbulent flow equations [34,35]. The combustion model uses the eddy-dissipation concept model (EDC) [19,36]. The pressure correction equation is solved by a PISO algorithm coupling with second-order upwind, which has an advantage in shock capture and accurately simulate detonation [19,37,38]. The 26-species 34-steps skeletal reaction mechanism of propane/air is selected [39]. This mechanism is believed to better reflect flow field characteristics, detonation wave structure and chemical kinetics of detonation.

2.3. Initial Parameters and Boundary Conditions

The flow field is initially filled with a mixture of propane oxygen and nitrogen at a temperature of 300K and a pressure of 0.128MPa. Among them, the mass fraction of propane is 9.4% and the oxygen was 34%, the rest is nitrogen. The ignition zone is simplified as a semicircle with a diameter of 15 mm, whose temperature is 2500 K. The pressure-outlet is chosen as the exit boundary condition of calculation domain. The walls are adiabatic and no-slip boundary conditions [40].

2.4. Grid-Independent and Model Validation

According to the geometric characteristics of the physical model, the quadrangular structured meshes are chosen in this paper. Selecting different mesh sizes (ranging from 0.5 mm to 2 mm). Figure 2 shows mesh size independence analysis. By comparing the variations of pressure with time at the same monitor point (P shows in Figure 1a), the monitoring pressure no longer changes significantly with decreasing mesh size when mesh size is reduced to 1 mm. Therefore, the parameters of 1 mm for mesh size is chosen in the following numerical simulation, which meets the requirements of independence.

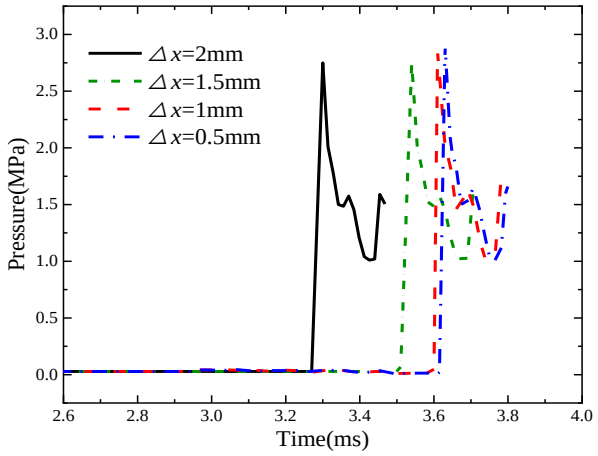

Figure 2. Mesh size independence analysis.

Experiments have been done to verify the validity of the numerical simulation. The experimental equipment schematic is shown in Figure 3. The PCB 113B24 pressure sensor is selected. Figure 4 compares the pressure curve of the experiment and numerical simulation at the same positions (P_2 and P_3 are located at 1035 mm and 1285 mm away from the left wall of detonation chamber), the pressure variation trends and peaks of them are very similar. According to Figure 4, we can confirm the experimental and simulated results are both the deflagration wave by the shape of the wave before the P_2, and there are the detonation waves at P_3. So DDT is completed between P_2 and P_3. In addition, the high detonation waves prove that the detonation initiation point is after P_2 [8,32]. The DDT time and distance of numerical simulation have good similarity with the experiment. Therefore, the validity of the numerical simulation used in this paper is proved.

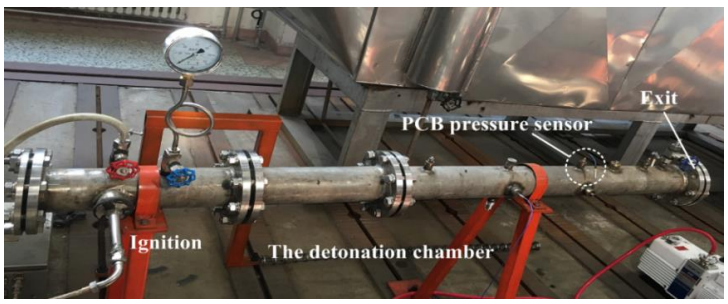

Figure 3. Schematic of the experience model.

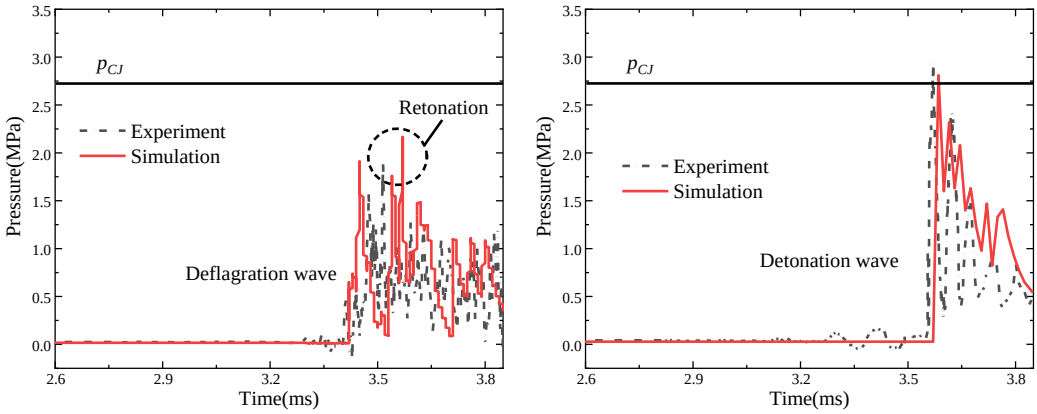

（**a**）P_2 （**b**）P_3

Figure 4. Pressure curves of experiment and numerical simulation.

Table 1 shows the comparison of theoretical and numerical detonation wave parameters. The theoretical parameters of detonation waves are obtained by chemical equilibrium with applications (NASA CEA) [41]. The value of the detonation parameters of this simulation method used in this paper is slightly larger than CEA, and the maximum deviation is only 3.4%. The comparison further verifies the validity of the numerical simulation method used in this paper.

Table 1. Comparisons of theoretical and numerical detonation wave parameters.

Parameters	Theoretical	Numerical	Deviation
p/p_1	21.15	21.87	3.40%
T/T_1	9.94	10.08	1.41%
V_{CJ} (m/s)	1904.4	1909.5	0.27%

Note: p is detonation front pressure. T is the detonation front temperature. p_1 is unburned pressure. T_1 is the unburned temperature. V_{CJ} is the detonation wave velocity.

3. Results Analysis and Discussion

The distance from the left wall of the detonation chamber to the position of detonation formation is defined as the initiation distance of DDT, represents by x_{DDT}. The time between ignition and hot jet propagating into the detonation chamber is defined as the time of hot jet formation, represents by t_{HJ}. The t_{TDC} is the time between the hot jet entering into the detonation chamber and the detonation initiation formation. So the time from ignition to detonation (t_{DDT}) is expressed as $t_{DDT} = t_{HJ} + t_{TDC}$. This paper mainly studies the influence of the ignition position inside the hot jet tube on the initiation distance and time of DDT. Before that, the mechanism of hot jet detonation initiation by the top ignition is necessary to be discussed firstly in detail.

3.1. Mechanism of Hot Jet Detonation Initiation

The hot jet detonation process is divided into three stages to study according to the combustion characteristic and temperature distribution. They are the stage of hot jet formation, vortex-flame interaction and detonation wave formation respectively. The flame propagation in hot jet tubes directly impacts the jet velocity and pressure, which might further affect the following formation of the final detonation wave. Therefore, the hot jet formation stage is discussed firstly. Figure 5 shows the hot jet formation in hot jet tube. Since the hot jet tube is a smooth tube, the flame-wall boundary layer interaction is an important factor affecting the flame propagation [42,43].

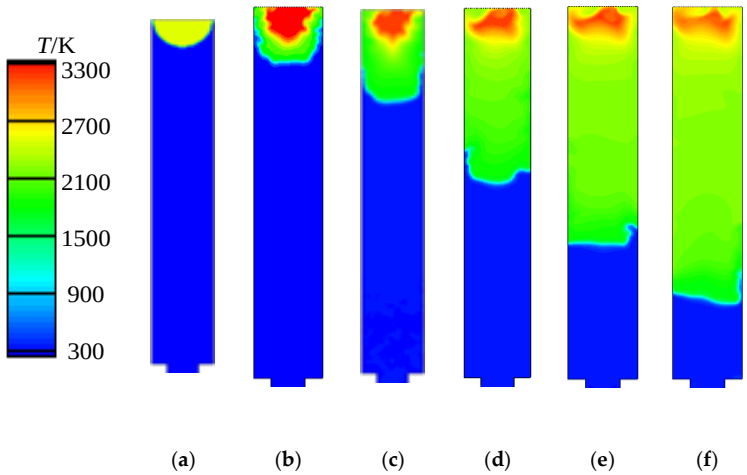

Figure 5. Hot jet formation process (**a**) t_{HJ} = 0 ms, (**b**) t_{HJ} = 0.15 ms, (**c**) t_{HJ} = 0.3 ms, (**d**) t_{HJ} = 0.6 ms, (**e**) t_{HJ} = 0.9 ms, (**f**) t_{HJ} = 1.2 ms.

From Figure 5a–c, high-temperature ignition source triggers laminar flame, and an expansion wave is generated during thermal mixture expansion [44]. Due to the obstructive effect of the wall boundary, the expansion waves are continuously superimposed and reflect on the flame. The flame wrinkles and the convex flame front propagates downstream at a laminar flow velocity of about 90m/s. In Figure 5d, since the pressure wave generated by the convex flame pushes unburned mixture to move towards near the wall, the high-density unburned mixture is formed near the wall and accelerates the flame propagation in this area. Then flame propagation speed near the wall increases rapidly, the contact area between flame and unburned mixture begins to decrease. Mass and thermal diffusion will also decrease. Flame front develops into an approximate plane, and flame propagation speed slows down.

Figure 6 shows the field of temperature and turbulent kinetic energy at 1.575 ms. The jet flame enters the detonation chamber, so t_{TDC} is assumed to be 0ms at this time. To further increase the jet velocity entering chamber, inspired by Ref. [18], the outlet of the hot jet tube has been designed as a sudden shrunken form as shown in Figure 6. Due to the narrow structure, convex flame propagates into the detonation chamber at a velocity of 333m/s. According to turbulent kinetic energy field, it is found that not only the flame front forms turbulence but also there are some high turbulence areas in the detonation chamber. The reason is that the pressure wave enters the detonation chamber ahead of flame and inevitably produces some disturbances in the detonation chamber. The Q criterion field is used to analyze these disturbances as shown in Figure 7. The Q criterion is defined by Hunt [45]:

$$Q = (\Omega_{ij}\Omega_{ji} - S_{ij}S_{ji})/2 \tag{1}$$

$$\Omega_{ij} = (\mu_{ij} - \mu_{ji})/2 \tag{2}$$

$$S_{ij} = (\mu_{ij} + \mu_{ji})/2 \tag{3}$$

where Ω_{ij} and S_{ij} are the rotate-rate and the strain-rate tensor of the velocity components, μ_{ij} and μ_{ji} are the partial derivatives of the velocity in the x and y-direction. The Q criterion can describe the structural characteristics of the vortex in the flow field.

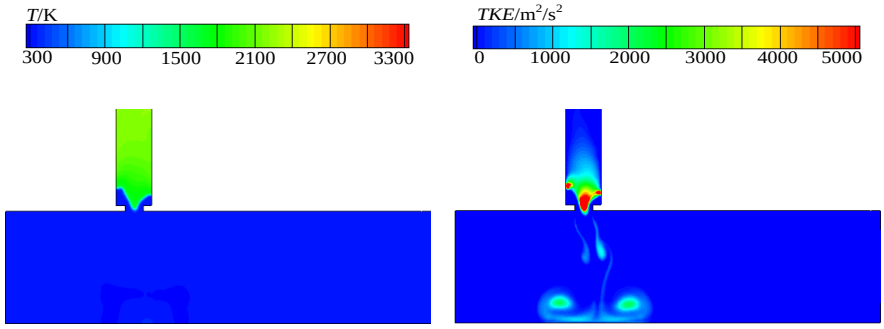

Figure 6. Temperature field and turbulent kinetic energy field at 1.575 ms.

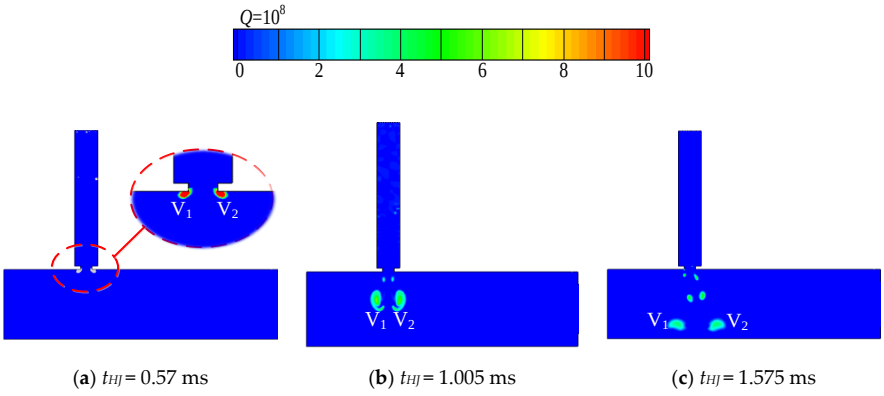

(**a**) t_{HJ} = 0.57 ms (**b**) t_{HJ} = 1.005 ms (**c**) t_{HJ} = 1.575 ms

Figure 7. Variations of *Q* criterion field.

Two vortexes (V_1 and V_2) can be found at the corners of the hot jet tube in Figure 7a. The pressure wave compresses the unburned mixture inside the hot jet tube into the detonation chamber. The velocity of the moving unburned mixture is significantly faster than the surrounding fluid. The intermittent velocity causes fluctuations, and the vortex occurs after the interface of the gas layer is destabilized [46]. The V_1 and V_2 continue to expand and move downstream in the detonation chamber with time. Comparing the *Q* criterion and turbulent kinetic energy at t_{HJ} = 1.575 ms (Figure 7c) and the *TKE* filed as shown in Figure 6, it is found that the vortex will form local turbulence.

The vortexes have formed before flame enters into the detonation chamber, so they inevitably affect the propagation of hot jet when flame propagates into the detonation chamber. Figure 8 shows the variations of temperature and *Q* criterion field, which reflects the interaction of vortex and jet flame. The O indicates the obstacle in the figure, and the O_i represents the *ith* obstacle. The gray area represents the vortex. At t_{TDC} = 0.03 ms, the jet flame propagates into the detonation chamber, the vertical distance between the largest scale vortexes (V_1 and V_2) and the flame front is 70 mm. From 0.03 ms to 0.24 ms, the flame surface area increases accordingly because of the sudden expansion of flow field structure and the small-scale vortexes. As the influence of the left wall, the jet flame propagates to the right in the detonation chamber. Flame reaches the down wall of the detonation chamber as shown in Figure 8d, and the V_1 and V_2 move to the sides by the hot reaction products.

Subsequently, the V_2 enhances the local turbulent fluctuation and entrains flame when t_{TDC} = 0.66 ms. Then V_2 accelerates the mixing between hot reaction products and cold unburned mixture [47], which is beneficial to promote the chemical reaction rate and diffusion rate of mass and heat. As a result, the vortex-flame interaction increases flame wrinkle surface area and accelerates the flame propagation. Since V_2 entrains the flame surface and V_1 does not touch the flame yet, the right flame surface increases more. Such actions lead to the formation of a "hook-type" flame as shown in Figure 8e. In addition, the vortex enhances the superposition between the pressure waves. The increasing pressure wave results in the stronger internal energy of unburned mixture, thus improving the flame propagation. According to Figure 8f, the right flame front propagates to the

first obstacle, and the V_1 begins to entrain the left flame. The unburned mixture propagates with the promotion of the high-temperature products and creates vortexes in the boundary layer of obstacle as the Kelvin-Helmholtz (K-H) instability [48].

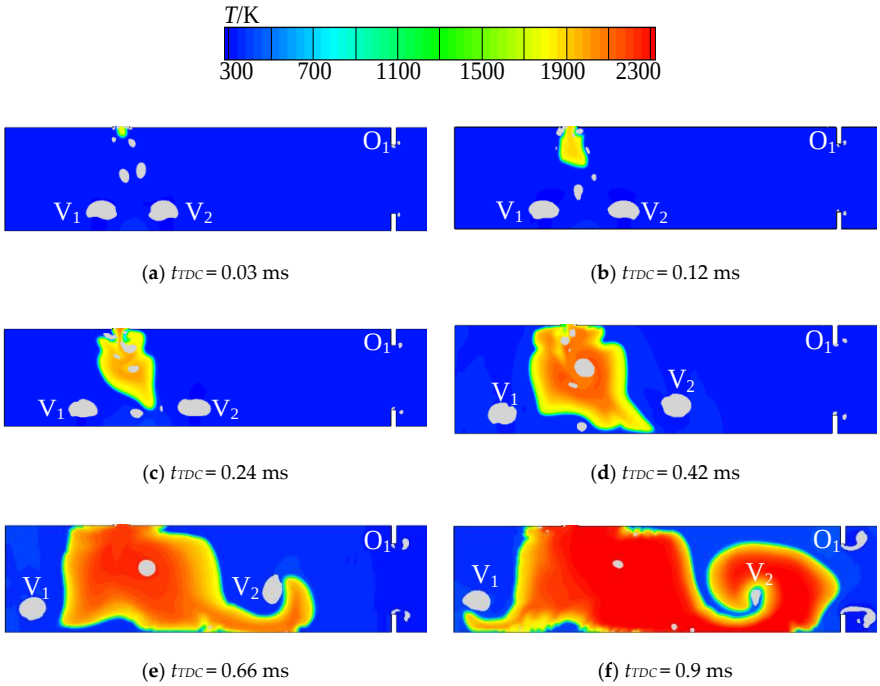

Figure 8. Interaction of jet flame and vortex in the detonation chamber.

As flame passes through the obstacles, the flame surface area, and flame propagation velocity both increase due to the Rayleigh-Taylor (RT) and K-H instabilities [49,50]. The flame becomes fast flame as shown in Figure 9 (a) [51], just arrives at the O_4. Figure 9 describes the formation of detonation wave by the variations of pressure and temperature field in detail. Obviously, a high-pressure zone occurs near the fourth obstacle at this moment. Pressure waves superimpose to form a shock in the leading edge of flame front. Since the leading shock compresses unburned mixture at front of flame to raises the temperature surrounding it, the chemical reaction and combustion are both promoted. Then plenty energies released from rapid combustion will strengthen the leading shock. This creates a positive feedback effect.

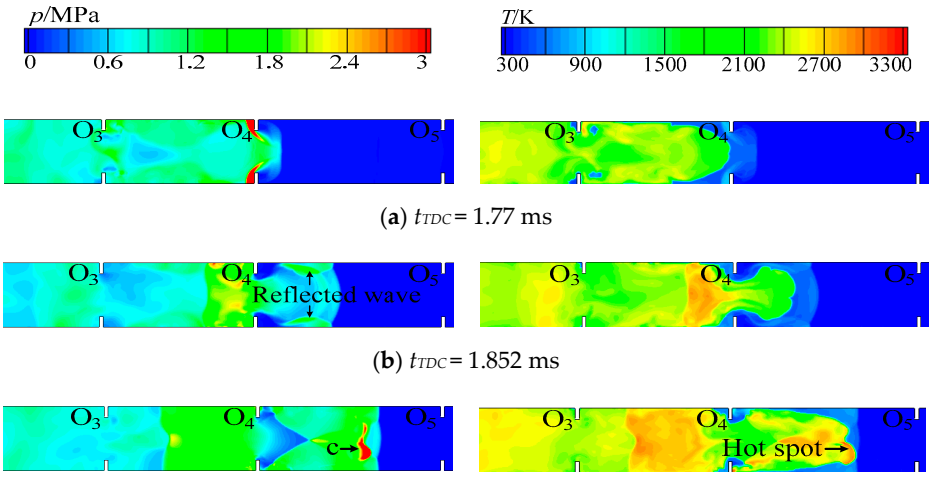

Figure 9. *Cont.*

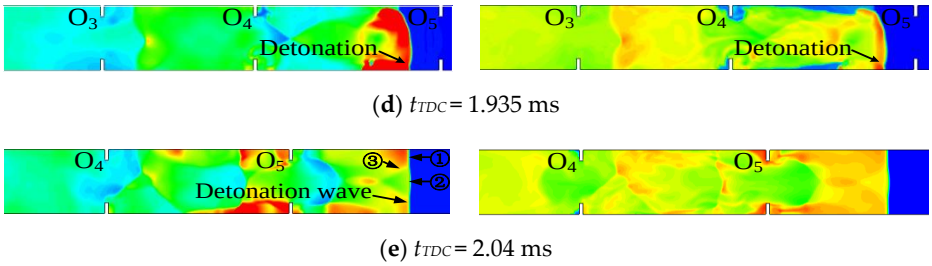

Figure 9. Variations of pressure and temperature field at detonation transition (DDT).

According to Figure 9b, the leading shock and flame pass the O_4, and the leading shock reflects from the wall. Then the leading and reflected waves collide at point "c" as shown in Figure 9c, the maximum pressure of "c" is over 6MPa. From the temperature field at this time, a hot spot is formed at the point "c". At t_{TDC} = 1.935 ms, the flame surface is coupled to the front shock, the hot spot develops to detonation wave at 1170 mm. The instabilities caused by internal combustion and walls lead to the generation of hot spots, which is the mechanism of the detonation wave formation [52]. The detonation wave coupled with shock and flame propagates downstream at velocity of 1909 m/s. Based on Figure 9e, ①Mach stem, ②incident shock, and ③transverse shock intersect to form the detonation wave system, the focus of the three shocks is called the "triple point" [53]. The key to the existence of stable and persistent detonation is that the "triple point" provides continuous energy to ensure the detonation wave velocity and propagate downstream successively.

3.2. The Influence of Ignition Position on the Hot Jet Detonation Initiation

Through the above study, it is found that the hot jet can form vortexes to accelerate flame propagation and promote DDT in the detonation chamber. However, the formation time of the hot jet is 44.87% of DDT time, which will greatly affect the performance of the detonation engine. In the previous paper, the ignition position inside the detonation chamber affects flame propagation [8]. So, the differences between top ignition and wall ignition are the following focus and research (ζ_Y = 0 mm as shown in Figure 1b. Figure 10 shows the time and distances to detonation initiation of two ignition positions. Simulation results clearly display that wall ignition can not only effectively reduce the t_{HJ}, but also shorten DDT time and distance. The top ignition t_{DDT} = 1.575 ms (t_{HJ}) + 1.935ms (t_{TDC}) = 3.51 ms, and x_{DDT} = 1170 mm. The wall ignition t_{DDT} = 1.005 ms (t_{HJ}) + 1.32 ms (t_{TDC}) = 2.325 ms, and x_{DDT} = 907 mm, the t_{DDT} and x_{DDT} are reduced by 33.76% and 22.48% comparing with top ignition.

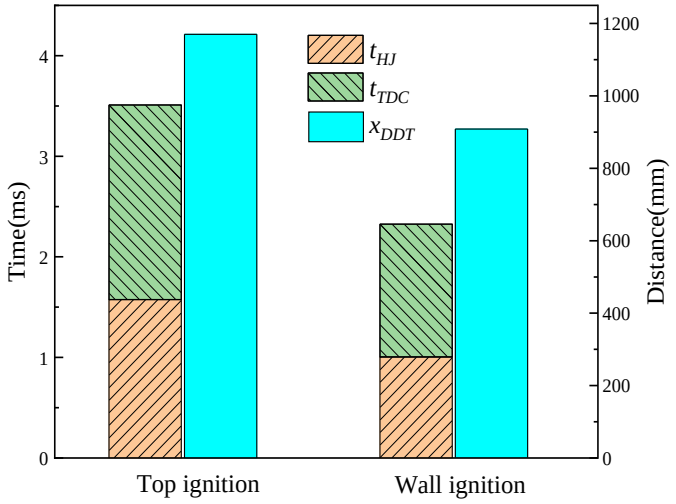

Figure 10. Time and distance to detonation initiation of top and wall ignition.

Figure 11 compares the flame propagation speed inside the jet tube of the two ignition positions, which can account for the reason of t_{HJ} reduction. In this figure, the distance represents the flame propagation distance in the hot jet tube, the left side is the ignition position, and the right side is the exit of the hot jet. The initial flame development of the two ignition positions is similar, then flame propagation speed of wall ignition is obviously higher than that of top ignition. Finally, the jet flame of wall ignition propagates into the detonation chamber at a velocity of 550m/s, which is about 1.65 times faster than that of top ignition.

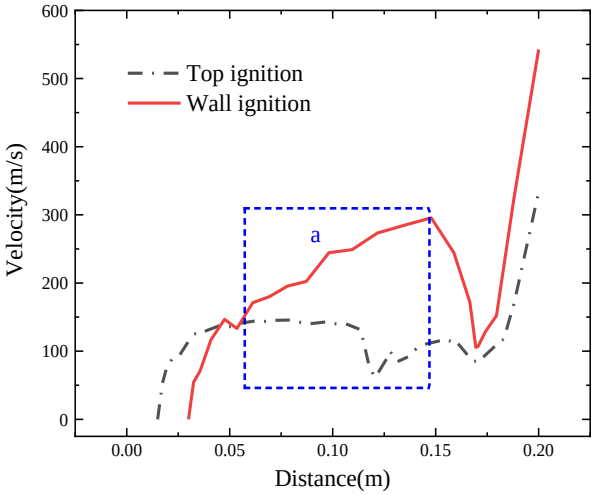

Figure 11. Flame propagation speed in the hot jet tube of two ignition positions.

Base on the "a" region of Figure 11, it is found that the flame propagation velocity of wall ignition is more than 2 times of the wall ignition. To investigate this issue, the variations of temperature field of wall ignition are studied as shown in Figure 12. At t_{HJ} = 0.3 ms, the pressure wave reaches right wall and then reflects. The reflected wave propagates to left, and it prevents the flame from contacting the right wall, thus ensuring the contact area between flame and unburned mixture. Comparing with Figure 5, there is more contact area between flame and unburned mixture in the flow field of wall ignition at this moment. More contact area releases more energy to increase the flame propagation speed. Therefore, the flame propagates faster and flame front reaches the exit of the jet tube in only 0.9 ms as shown in Figure 12c, the propagation distance is significantly farther than the flame of Figure 5e. Then flame front transforms from "fingertip" to "planar" shape. Flame contacting with wall results in reducing the contact area between flame and unburned mixture, thus slowing down the flame propagation speed. However, the flame propagation speed of wall ignition is faster than that of top wall, and wall ignition takes only 1.005 ms to form a hot jet into the detonation chamber.

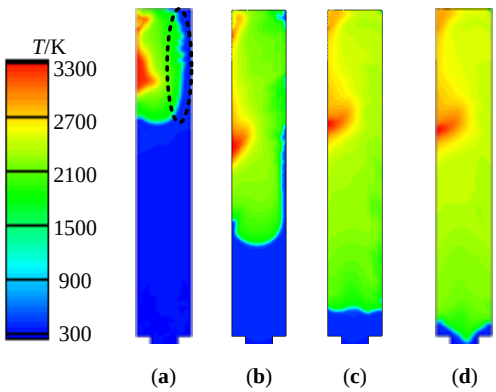

Figure 12. Variations of temperature field of the wall ignition (**a**) t_{HJ} = 0.3 ms, (**b**) t_{HJ} = 0.6 ms, (**c**) t_{HJ} = 0.9 ms, (**d**) t_{HJ} = 1.005 ms.

The jet pressure also affects the jet flame propagation into the detonation chamber, so a detailed comparison of the jet pressure changes with time at the center point of the hot jet tube is shown in Figure 13. The first pressure peak appears at 0.5 ms. The pressure peak of wall ignition is 1.35 times that of top ignition. Subsequently, the pressure of wall ignition is always higher than the top ignition. The second pressure peak appears at 0.75 ms and the peak value can reach 0.2 MPa. The jet flame of wall ignition enters detonation chamber with 0.1 MPa at 1.005 ms, which is obviously higher than 0.06 MPa of top ignition. The average pressure of the wall ignition is twice than top ignition due to more intense burning and wave superimposition. On the basis of above discussions of jet velocity, it is found wall ignition brings a faster hot jet with higher pressure.

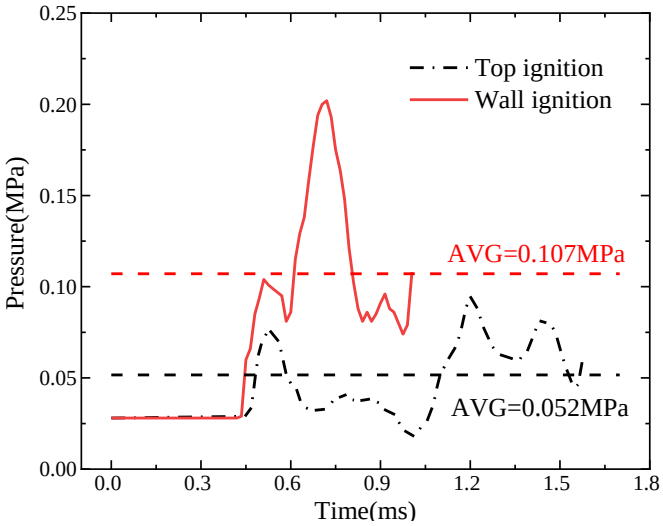

Figure 13. Pressure changes of two ignition positions at the exit of the hot jet tube.

In order to understand flame propagation and detonation wave formation of the two ignition positions. The comparison of flame propagation speed is shown in Figure 14. The trend of these two flame propagations is generally the same due to the same structure, but the flame propagation of wall ignition is substantially faster than that of top ignition. The wall ignition forms a detonation wave first. According to the characteristics of the flame speed, this figure is divided into two regions to study. (**I**) In this region, the vortex entrains the jet flame to increase the flame speed before the first obstacle. (**II**) The flame constantly accelerates because of the obstacles, and eventually forms a detonation wave.

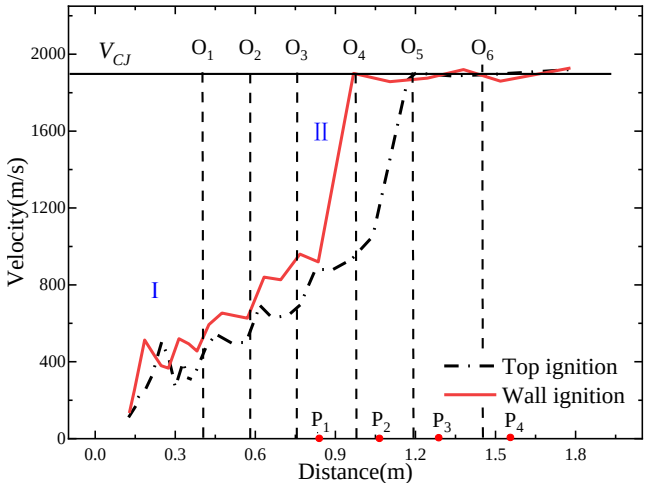

Figure 14. Flame propagation speed in the detonation chamber.

In the first region, the flame propagation speed of wall ignition increases significantly fast and remains at big speed. Except for the area around 0.23 m (the V_1 entrains the flame of top ignition as shown in Figure 8e), the flame speed of wall ignition is always faster than that of top ignition. Figure 15 displays the variations of temperature and Q criterion field of wall ignition before the first obstacle to investigate why the flame speed of wall ignition is faster. Comparing with Figure 8a, it can be seen that the scale of the vortexes (V_1 and V_2) is larger at t_{TDC} = 0.03 ms due to the higher jet pressure and the faster jet velocity. Additionally, the reducing formation time of hot jet results in short moving time of V_1 and V_2, so the vertical distance between the vortexes (V_1 and V_2) and the flame front is only 14 mm, which is obviously closer than that of top ignition. Base on Figure 15b,c, flame quickly contacts the vortexes (V_1 and V_2). The two same scale vortexes (V_1 and V_2) simultaneously entrain the flame. Then flame temperature and wrinkling surface both increase rapidly and a symmetrical "mushroom-shaped" flame is produced at t_{TDC} = 0.24 ms. Subsequently, flame reaches the first obstacle by only 0.66 ms, which is 26.67% less than top ignition. Moreover, a large amount of mixture is burned to release energy, which is more conducive to the next acceleration of the flame. Comparing with Figure 8, vortex entrains flame earlier and the scale of vortex is significantly larger, so the flame propagation speed of wall ignition is faster than that of top ignition.

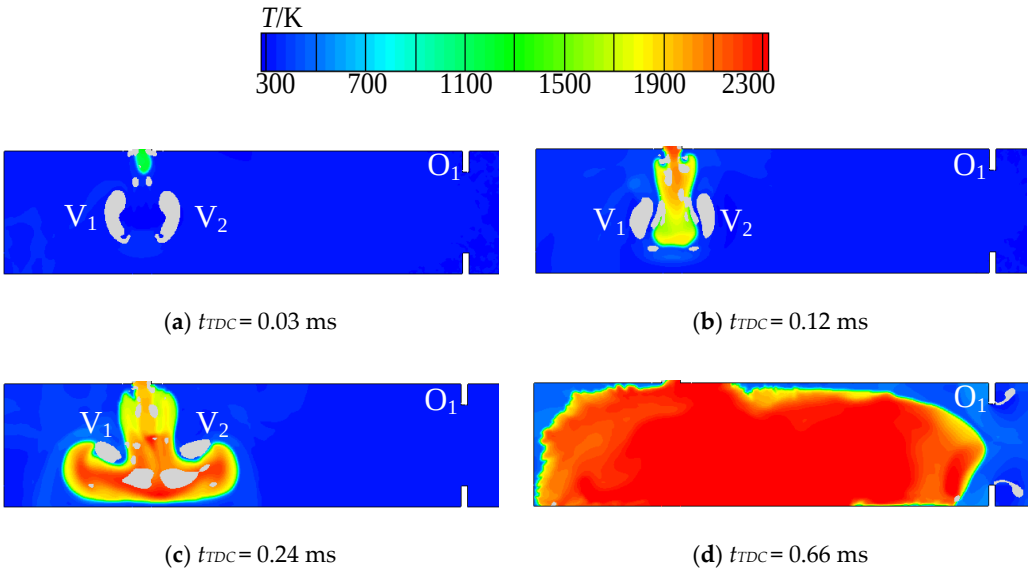

(**a**) t_{TDC} = 0.03 ms (**b**) t_{TDC} = 0.12 ms

(**c**) t_{TDC} = 0.24 ms (**d**) t_{TDC} = 0.66 ms

Figure 15. Variations of temperature and Q criterion field of wall ignition.

In the second region, as the flame propagation speed of wall ignition is faster than that of top ignition when the flame passes the first obstacle, its flame propagation speed is always faster at the second stage as shown in Figure 14. Subsequently, the wall ignition forms a detonation wave in advance as shown in Figure 16. Wall ignition burns more intensely at the early stage in the detonation chamber, so superposition of pressure waves is more intense. According to Figure 16a, two high-intensity reflected waves have been formed before the third obstacle. Then the reflected waves and leading shock collide at point "c", and a hot spot is formed which is significantly ahead of the top ignition. The high temperature and pressure point accelerate energy release to accelerate DDT which precedes than top ignition. The triple point(① Mach stem, ② incident shock, and ③ transverse shock) is promoted for the case of ignition at the wall because of the higher pressure waves and flame strength than that of top ignition. On the basis of above discussions, it is found that wall ignition forms a fast hot jet with high pressure, shortens the formation time of hot jet, and forms large-scale vortexes. These all contribute to accelerating flame and superimposing pressure waves. So the DDT distance and time of wall ignition are significantly shorter than top ignition.

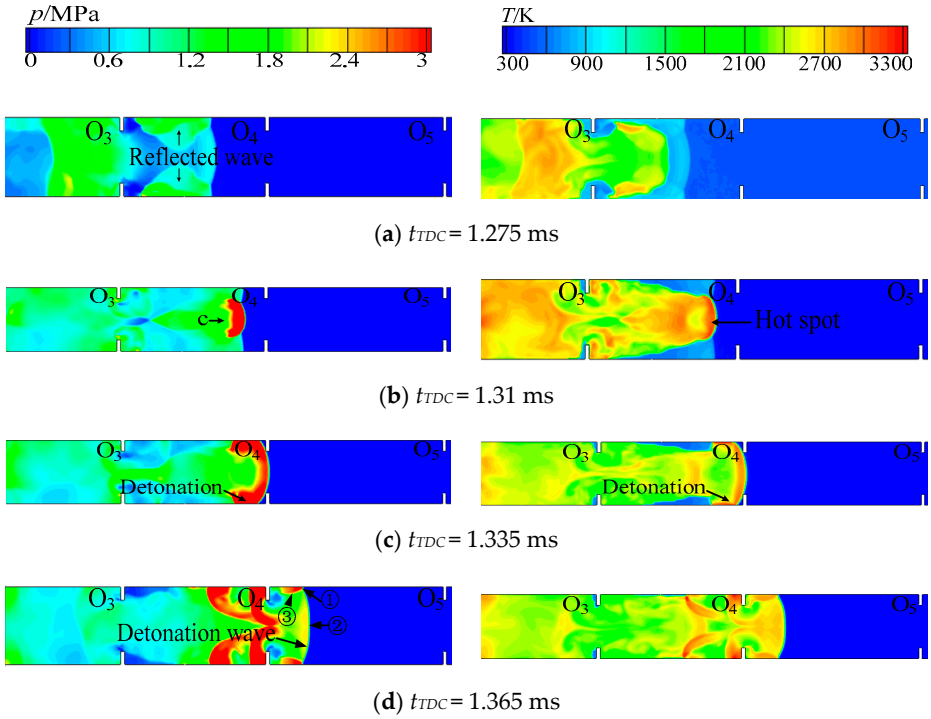

Figure 16. Variations of pressure and temperature field at deflagration-to-detonation transition (DDT) of wall ignition.

3.3. Optimization of Ignition Position

Through the above study, it is found that wall ignition is more conducive to the acceleration of DDT. To further study the performance advantage of wall ignition, the effect of different wall ignition positions on DDT is studied in this section. The ignition positions of ζ_Y = 30 mm, 60 mm, 90 mm, 120 mm, and 150 mm are simulated as well. Figure 17 displays the jet velocity and pressure of different ignition positions when jet flame front enters into the detonation chamber. Since too big ζ_Y results in less mixture combustion in the jet tube, thus weakening the jet velocity and pressure. When ζ_Y is large, the jet velocity and pressure are both relatively small. As ζ_Y increases, the jet velocity maintains at about 550 m/s and then an obvious reduction occurs. The jet pressure increases firstly and then weakens with increase of ζ_Y, and the highest peak is observed ζ_Y = 30 mm. The pressure wave is reflected not only on the left and right walls but also on the top of jet tube [46]. Therefore, it is more advantageous to obtain larger jet pressure when ζ_Y = 30 mm.

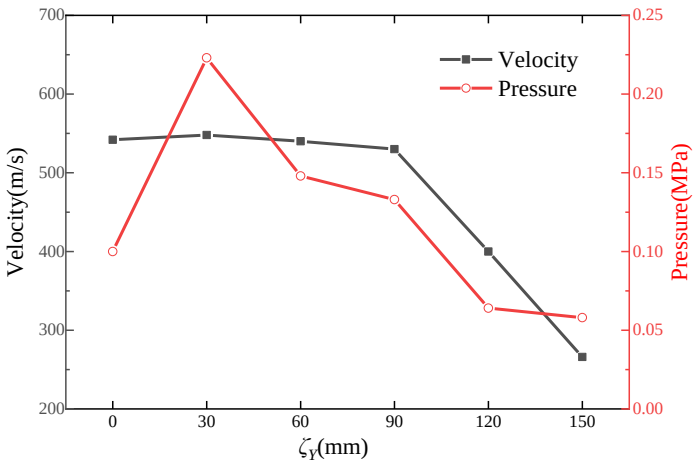

Figure 17. Jet velocity and pressure of different ignition positions.

Then jet flame propagates into the detonation chamber, flame wrinkling surface area and propagation speed both increase by vortexes and obstacles. In order to compare the flame propagation in the detonation chamber for different ignition positions, distributions of pressure and temperature on the axis at different ignition positions at t_{TDC} = 1.44 ms are shown in Figure 18 ($\zeta_Y \leq 60$ mm) and Figure 19 ($\zeta_Y \geq 90$ mm). Since the fast hot jet, flame and pressure propagate farther in Figure 18 than those of Figure 19. The propagation distances of flame and pressure are farthest when ζ_Y = 30 mm. The values of leading shock already meet the detonation parameter in Figure 18, and flame front couple with the leading shock, so the detonation wave has been formed in the detonation chamber.

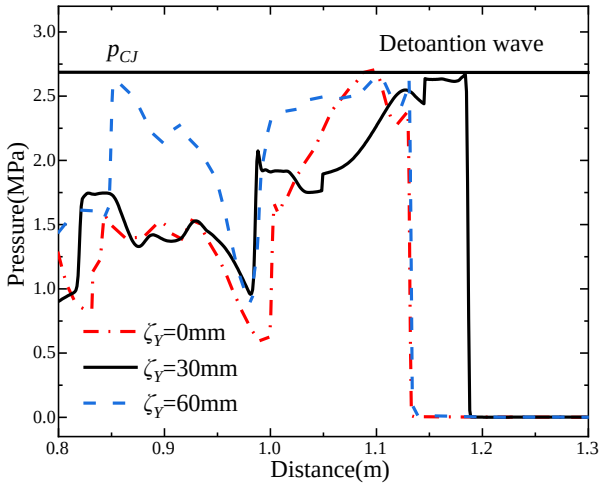

(**a**) Pressure

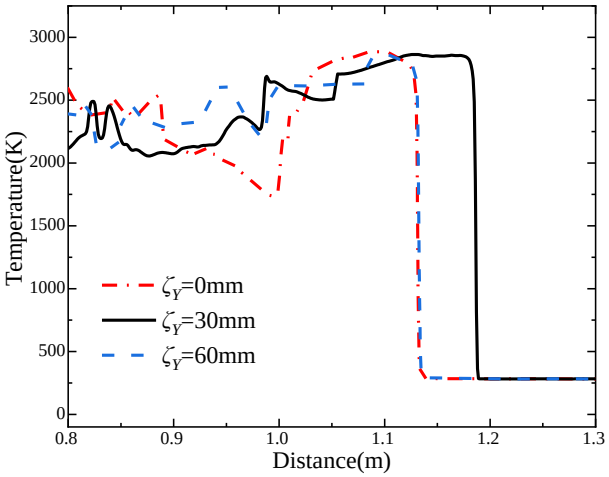

(**b**) Temperature

Figure 18. Distributions of (**a**) pressure and (**b**) temperature of $\zeta_Y \leq 60$ mm at t_{TDC} = 1.44 ms.

Base on Figure 19, the propagation distance of pressure wave and flame decrease as ζ_Y increasing, and the pressure wave propagate slightly further than flame front. It is clearly seen that the pressure of deflagration wave is weak at this time, and value of pressure wave decreases as ζ_Y increasing. The pressure of ζ_Y = 150 mm is obviously lower than other ignition positions, which does not form the leading shock.

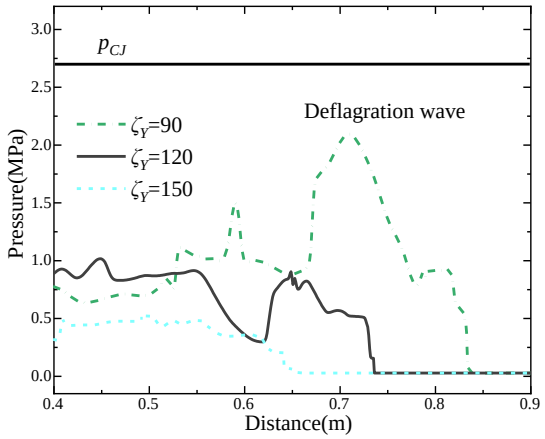

(**a**) Pressure

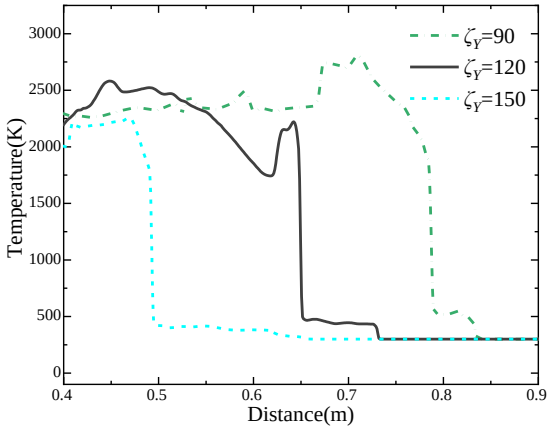

(**b**) Temperature

Figure 19. Distributions of (**a**) pressure and (**b**) temperature of $\zeta_Y \geq 90$ mm at $t_{TDC} = 1.44$ ms.

Figure 20 shows the DDT distance and time of different ignition positions. The t_{DDT} ($t_{HJ} + t_{TDC}$) and x_{DDT} both decrease firstly and then increase with ζ_Y increasing. The ignition position is near the exit of the hot jet tube when the ζ_Y is big, so the t_{HJ} is small. However, the reduction of jet intensity leads to a long time and distance to complete DDT. As the jet velocity and pressure are the largest at $\zeta_Y = 30$ mm, the shortest x_{DDT} is 810 mm and the fastest t_{DDT} is 2.055 ms at this time.

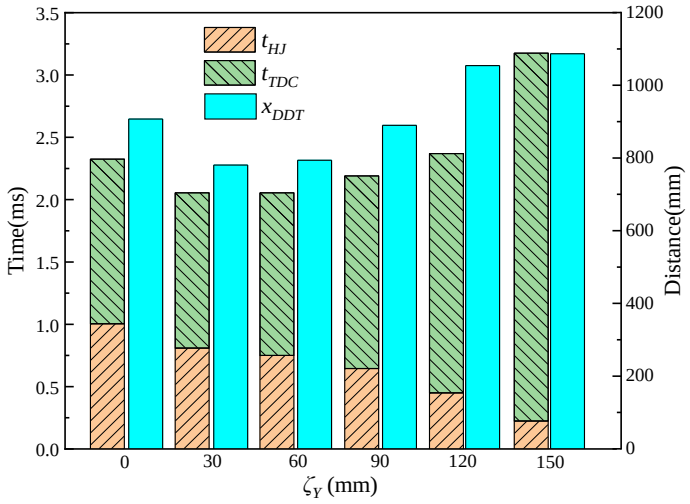

Figure 20. DDT distance and time of different ignition positions.

4. Conclusions

This paper uses a two-dimensional numerical simulation method to study the effect of different ignition positions inside the hot jet tube on the distance and time of detonation initiation. The hot jet formation, the vortex-flame interaction and character of the initiation time and distance to detonation initiation are analyzed in detailed. The primary conclusions of this study include as following:

(1) The mechanism of the hot jet detonation initiation is fast jet flame and the vortex-flame interaction. The vortexes increase turbulence intensity to accelerate blending between the unburned mixture and high-temperature products and increase superposition of the waves. Therefore, the increasing flame wrinkling surface area results in faster mass and energy release, thus increasing the flame propagation speed and accelerating DDT.

(2) Wall ignition is significantly better than top ignition on DDT. When the ignition position changes from the top to the wall inside the hot jet tube, the DDT distance and time are both showing an obvious reduction. Two differences should be paid special attention: one is the vortexes entrain flame early. Another is the scale of vortex is big and two large-scale vortexes simultaneously entrain flame. The reason mainly lies in the formation of hot jet with stronger intensity in cause of wall ignition.

(3) The different wall ignition positions also affect the detonation wave formation. The t_{DDT} and x_{DDT} all reduce firstly and then increase with ζ_Y increasing. The shortest x_{DDT} is 810 mm and the fastest t_{DDT} is 2.055 ms at ζ_Y = 30 mm. This is because not only the jet velocity is ensured to be about 550 m/s, but also the jet pressure is the largest due to the pressure wave is reflected on the wall and top of the hot jet tube.

Author Contributions: Conceptualization, H.Z.; formal analysis, S.L.; methodology, N.Z.; investigation, X.C.; writing—original draft preparation, X.J.; writing—review and editing, Z.L.

Funding: The authors would like to acknowledge the Fundamental Research Funds for the Central Universities (Grant No. HEUCFP201719) for supporting this work.

Conflicts of Interest: The authors declared that there was no conflict of interest.

References

1. Kailasanath, K. Review of propulsion applications of detonation waves. *AIAA J.* **2000**, *38*, 1698–1708. [CrossRef]
2. Zheng, H.T.; Qi, L.; Zhao, N.B.; Li, Z.M.; Liu, X. A Thermodynamic Analysis of the Pressure Gain of Continuously Rotating Detonation Combustor for Gas Turbine Cycle Performance. *Appl. Sci.* **2018**, *8*, 535. [CrossRef]
3. Meng, Q.; Zhao, N.B.; Zheng, H.T.; Yang, J.L.; Qi, L. Numerical investigation of the effect of inlet mass flow rates on H2/air non-premixed rotating detonation wave. *Int. J. Hydrog. Energy* **2018**, *43*, 13618–13631. [CrossRef]
4. Sun, C.W.; Zheng, H.T.; Li, Z.M.; Zhao, N.B.; Qi, L.; Guo, H.B. Effects of Diverging Nozzle Downstream on Flow Field Parameters of Rotating Detonation Combustor. *Appl. Sci.* **2019**, *9*, 4259. [CrossRef]
5. Driscoll, R.; George, A.S.; Munday, D.; Gutmark, E.J. Optimization of a multiple pulse detonation engine-crossover system. *Appl. Eng.* **2016**, *96*, 463–472. [CrossRef]
6. Frolov, S.M.; Smetanyuk, V.A.; Gusev, P.A.; Koval, A.S.; Nabatnikov, S.A. How to utilize the kinetic energy of pulsed detonation products. *Appl. Therm. Eng.* **2019**, *147*, 728–734. [CrossRef]
7. Wang, Y.; Wang, K.; Fan, W.; He, J.N.; Zhang, Y.; Zhang, Q.B.; Yao, K.G. Experimental study on the wall temperature and heat transfer of a two-phase pulse detonation rocket engine. *Appl. Therm Eng.* **2017**, *114*, 387–393. [CrossRef]
8. Sorin, R.; Zitoun, R.; Desbordes, D. Optimization of the deflagration to detonation transition: Reduction of length and time of transition. *Shock Waves* **2006**, *15*, 137–145. [CrossRef]
9. Harris, P.; Farinaccio, R.; Stowe, R.; Higgins, A.; Thibault, P.; Laviolette, J. The effect of DDT distance on impulse in a detonation tube. In Proceedings of the 37th AIAA/ASME/SAE/ASEE Joint Propulsion Conference & Exhibit, AIAA 2001-3467, Salt Lake City, UT, USA, 8–11 July 2001.

10. Sorin, R.; Zitoun, R.; Khasainov, B.; Desbordes, D. Detonation diffraction through different geometries. *Shock Waves* **2009**, *19*, 11–23. [CrossRef]
11. Jackson, S.; Shepherd, J. Initiation systems for pulse detonation engines. In Proceedings of the 38th AIAA/ASME/SAE/ASEE Joint Propulsion Conference & Exhibit, AIAA 2002-3627, Indianapolis, IN, USA, 7–10 July 2002.
12. Kellenberger, M.; Ciccarelli, G. Advancements on the propagation mechanism of a detonation wave in an obstructed channel. *Combust. Flame* **2018**, *159*, 195–209. [CrossRef]
13. Li, J.; Zhang, P.; Yuan, L.; Pan, Z.; Zhu, Y. Flame propagation and detonation initiation distance of ethylene/oxygen in narrow gap. *Appl. Therm. Eng.* **2017**, *110*, 1274–1282. [CrossRef]
14. Chambers, J.; Ahmed, K. Turbulent flame augmentation using a fluidic jet for Deflagration-to-Detonation. *Fuel* **2017**, *199*, 616–626. [CrossRef]
15. Zhao, S.; Fan, Y.; Lv, H.; Jia, B. Effects of a jet turbulator upon flame acceleration in a detonation tube. *Appl. Therm. Eng.* **2017**, *115*, 33–40. [CrossRef]
16. Wang, F.; Kuthi, A.; Gundersen, M. Technology for transient plasma ignition. In Proceedings of the 43th AIAA Aerospace Sciences Meeting & Exhibit, AIAA 2005-951, Reno, NV, USA, 10–13 January 2005.
17. Xiao, H.; Oran, E.S. Shock focusing and detonation initiation at a flame front. *Combust. Flame* **2019**, *203*, 397–406. [CrossRef]
18. Shimada, H.; Kenmoku, Y.; Sato, H.; Hayashi, A.K. A new ignition system for pulse detonation engine. In Proceedings of the 42th AIAA/ASME/SAE/ASEE Joint Propulsion Conference & Exhibit, AIAA 2004-308, Reno, NV, USA, 5–8 January 2004.
19. Zhao, W.; Han, Q.X.; Zhang, Q. Experimental investigation on detonation initiation with a transversal hot jet. *Combust. Explos. Shock Waves* **2013**, *49*, 171–177. [CrossRef]
20. Brophy, C.; Sinibaldi, J.; Damphousse, P. Initiator performance for liquid-fueled pulse detonation engines. In Proceedings of the 40th AIAA Aerospace Sciences Meeting & Exhibit, AIAA 2002-472, Reno, NV, USA, 14–17 January 2002.
21. Brophy, C.; Werner, S.; Sinibaldi, J. Performance characterization of a valveless pulse detonation engine. In Proceedings of the 41th AIAA Aerospace Sciences Meeting & Exhibit, AIAA 2003-1344, Reno, NV, USA, 6–9 January 2003.
22. Ishii, K.; Tanaka, T. A study on jet initiation of detonation using multiple tubes. *Shock Waves* **2005**, *14*, 273–281. [CrossRef]
23. Ishii, K.; Akiyoshi, T.; Gonda, M.; Murayama, M. Effects of flame jet configurations on detonation initiation. *Shock Waves* **2009**, 239–244.
24. Saretto, S.R.; Lee, S.Y.; Conrad, C.; Brumberg, J.; Pal, S.; Stantoro, R.J. Predetonator to thrust tube detonation transition studies for multi-cycle PDE applications. In Proceedings of the 39th AIAA/ASME/SAE/ASEE Joint Propulsion Conference & Exhibit, AIAA 2003-4825, Huntsville, AL, USA, 20–23 July 2003.
25. Conrad, C.; Saretto, S.R.; Lee, S.Y.; Stantoro, R.J. Studies of Overdriven Detonation Wave Transition in a Gradual Area Expansion for PDE Applications. In Proceedings of the 40th AIAA/ASME/SAE/ASEE Joint Propulsion Conference & Exhibit, AIAA 2004-3397, Fort Lauderdale, FL, USA, 11–14 July 2004.
26. He, J.; Fan, W.; Chi, Y.; Zheng, j.; Zhang, W. A Comparative Study on Millimeter-scale Hot jet and Detonation Diffraction in a Rectangular Chamber. In Proceedings of the 21th AIAA International Space Planes and Hypersonics Technologies Conference, AIAA 2017-2149, Xiamen, China, 6–9 March 2017.
27. Wang, Z.; Zhang, Y.; Chen, X.; Liang, Z.; Zheng, L. Investigation of Hot Jet Effect on Detonation Initiation Characteristics. *Combust. Sci. Technol.* **2017**, *189*, 498–519. [CrossRef]
28. Kumar, K. Vented combustion of hydrogen-air mixtures in a large rectangular volume. In Proceedings of the 44th AIAA Aerospace Sciences Meeting & Exhibit, AIAA 2006-375, Reno, NV, USA, 9–12 January 2006.
29. Kindracki, J.; Kobiera, A.; Rarata, G.; Wolanski, P. Influence of ignition position and obstacles on explosion development in methane–air mixture in closed vessels. *J. Loss Prev. Process Ind.* **2007**, *20*, 551–561. [CrossRef]
30. Xiao, H.; Duan, Q.; Jiang, L.; Sun, J. Effects of ignition location on premixed hydrogen/air flame propagation in a closed combustion tube. *Int. J. Hydrog. Energy* **2014**, *39*, 8557–8563. [CrossRef]
31. Peng, Z.; Weng, C. Numerical Calculation of Effect of Plasma Ignition on DDT. *Combust Sci. Technol.* **2011**, 1.
32. Blanchard, R.; Arndt, D.; Grätz, R.; Scheider, S. Effect of ignition position on the run-up distance to DDT for hydrogen–air explosions. *J. Loss Prev. Process Ind.* **2011**, *24*, 194–199. [CrossRef]

33. Goodwin, G.B.; Houim, R.W.; Oran, E.S. Effect of decreasing blockage ratio on DDT in small channels with obstacles. *Combust. Flame* **2016**, *173*, 16–26. [CrossRef]
34. Perera, I.; Wijeyakulasuriya, S.; Nalim, R. Hot combustion torch jet ignition delay time for ethylene-air mixtures. In Proceedings of the 49th AIAA Aerospace Sciences Meeting including the New Horizons Forum and Aerospace Exposition, AIAA 2011-95, Orlando, FL, USA, 4–7 January 2011.
35. Luo, C.; Zanganeh, J.; Moghtaderi, B. A 3D numerical study of detonation wave propagation in various angled bending tubes. *Fire Safety J.* **2016**, *86*, 53–64. [CrossRef]
36. Zhang, Z.; Li, Z.; Wu, Y.; Bao, X. Numerical Studies of Multi-Cycle Detonation Induced by Shock Focusing. In Proceedings of the Asia-pacific International Symposium on Aerospace Technology, Toyama, Japan, 25–27 October 2016.
37. Qin, Y.; Yu, J.; Gao, G. Performance studies of annular pulse detonation engine ejectors. *J. Aerosp. Power* **2011**, *26*, 25–41.
38. Zhang, Z.; Li, Z.; Dong, G. Numerical studies of multi-cycle acetylene-air detonation induced by shock focusing. *Procedia Eng.* **2015**, *99*, 327–331. [CrossRef]
39. Petrova, M.; Varatharajan, B.; Williams, F. Theory of Propane Autoignition. In Proceedings of the 42th AIAA Aerospace Sciences Meeting & Exhibit, AIAA 2004-1325, Reno, NV, USA, 5–8 January 2004.
40. Goodwin, G.B.; Houim, R.W.; Oran, E.S. Shock transition to detonation in channels with obstacles. *Proc. Combust. Inst.* **2017**, *36*, 2717–2724. [CrossRef]
41. CEARUN. Available online: https://cearun.grc.nasa.gov (accessed on 5 February 2004).
42. Kuznetsov, M.; Alekseev, V.; Matsukov, I.; Dorofeev, S. DDT in a smooth tube filled with a hydrogen–oxygen mixture. *Shock Waves* **2005**, *14*, 205–215. [CrossRef]
43. Bychkov, V.; Fru, G.; Eriksson, L.E.; Petchenko, A. Flame acceleration in the early stages of burning in tubes. *Combust. Flame* **2007**, *150*, 263–276. [CrossRef]
44. Landau, L.D.; Lifshitz, E.M. *Course of Theoretical Physics*; Elsevier: Amsterdam, The Netherlands, 2013.
45. Hunt, J.C.R.; Wray, A.A.; Moin, P. Eddies, streams, and convergence zones in turbulent flows. Cent Turbul Res Report CTR-S88. 1988, pp. 193–208. Available online: https://www.researchgate.net/publication/234550074_Eddies_streams_and_convergence_zones_in_turbulent_flows (accessed on 29 October 2019).
46. Fan, J.; Zhang, Y.; Wang, D. Large-eddy simulation of three-dimensional vortical structures for an impinging transverse jet in the near region. *J. Hydrodyn.* **2007**, *19*, 314–321. [CrossRef]
47. Ahmed, U.; Prosser, R. Modelling Flame turbulence interaction in RANS simulation of premixed turbulent combustion. *Combust. Theory Model.* **2016**, *20*, 34–57. [CrossRef]
48. Ciccarelli, G.; Dorofeev, S. Flame acceleration and transition to detonation in ducts. *Prog. Energy Combust. Sci.* **2008**, *34*, 499–550. [CrossRef]
49. Gamezo, V.N.; Ogawa, T.; Oran, E.S. Flame acceleration and DDT in channels with obstacles: Effect of obstacle spacing. *Combust. Flame* **2008**, *155*, 302–315. [CrossRef]
50. Ott, J.D.; Oran, E.S.; Anderson, J.D. A mechanism for flame acceleration in narrow tubes. *AIAA J.* **2003**, *41*, 1391–1396. [CrossRef]
51. Kagan, L.; Sivashinsky, G. Parametric transition from deflagration to detonation: Runaway of fast flames. *Proc. Combust. Inst.* **2017**, *36*, 2709–2715. [CrossRef]
52. Wang, Z.; Qi, Y.; He, X.; Wang, J.; Shuai, S.; Law, C.K. Analysis of pre-ignition to super-knock: Hotspot-induced deflagration to detonation. *Fuel* **2015**, *144*, 222–227. [CrossRef]
53. Massa, L.; Austin, J.; Jackson, T. Triple point shear-layers in gaseous detonation waves. *J. Fluid Mech.* **2007**, *586*, 205–248. [CrossRef]